

Results obtained with ABLA07

M. Valentina Ricciardi¹, Aleksandra Kelić¹, Karl-Heinz Schmidt¹

¹ GSI Helmholtzzentrum für Schwerionenforschung, 64291 Darmstadt, Germany

Email contact of main author: m.v.ricciardi@gsi.de

Abstract. The de-excitation code ABLA has been continuously developed in the last years, guided by the empirical knowledge gained in a campaign of spallation and fragmentation experiments performed at GSI, Darmstadt. The better insight into the reaction mechanisms lead to a highly improved version of the code, namely ABLA07, whose physical content and technical algorithms are described in great detail in the authors' contribution to the proceedings of the "Joint ICTP-IAEA Advanced Workshop on Model Codes for Spallation Reactions," held in Trieste, Italy, 4-8 January 2008. This paper presents some significant examples of the performances of the ABLA07 code, especially focusing on the interplay between the modeling of the collision stage and the de-excitation process.

1. Introduction

Spallation reactions are often described as a two-stage process. In the first stage, the collision between the target and the projectile is modeled. There are several types of models for the first-stage of the reaction, which have different degrees of sophistications: from microscopic codes, like pure quantum-mechanical dynamical codes, quantum-molecular dynamics codes, transport-equation codes, and intra-nuclear-cascade codes (see ref. [1] for more), to macroscopic abrasion-like codes. The most important feature is that after the first stage the remnant nucleus can have changed its neutron and proton content, acquired a certain excitation energy, linear and angular momentum. The second stage treats the further evolution of the remnant nucleus, namely its de-excitation down to the cold experimentally-observable final fragment. There are experimental indications that this stage resembles the evaporation of molecules from a drop of heated liquid. For this reason, the second stage is always treated by means of statistical models applying thermodynamical pictures.

Technically, the modeling of the first stage of the reaction is completely independent from the modeling of the second stage. Different first-stage codes can be coupled to different second-stage codes. In this paper, we discuss the performances of the de-excitation code ABLA07[2]. To this purpose, we will present the results of simulations obtained using INCL4 [3], ISABEL [4], and BURST [5,6] as first-stage codes, coupled with ABLA07 as second-stage code.

2. The codes

Both INCL4 and ISABEL are based on intra-nuclear cascade (INC) models. Please find detailed descriptions of the codes in ref. [3,4]. The BURST model is included in ABRABLA nuclear-reaction code, developed at GSI, Darmstadt. ABRABLA consists of the ABRA abrasion model for the first-stage of the reaction and of the ABLA code, for the second stage. The ABRA model was originally developed [7] to treat nucleus-nucleus collisions. Later on, ABRA was extended to treat also nucleon-nucleus interactions, by including an analytical model named BURST [5, 6], based on a parameterization of the results predicted by INCL.

The ABLA code is named after the "ablation" process. The starting point of ABLA is the thermalised nucleus. In ABLA, the compound nucleus undergoes the statistical de-excitation. Statistical multifragmentation, sequential evaporation, very asymmetric binary splitting,

dynamical fission and gamma decay are consistently treated by the code. Several people contributed to the development of ABLA in the last decade. Please find a comprehensive description of the latest version of the code, ABLA07, in the IAEA report [2] and therein quoted references. With respect to older versions, it covers all phenomena relevant for the production of final fragments. In order to ensure a good predictive power, the physical processes are always described by appropriate theories (when existing), avoiding parameterizations. Please note that, while abrasion and INC codes – modeling the first stage of the reaction – are applicable only well above the Fermi energy, ABLA07 is a valid description of the de-excitation stage starting at any energy and for any compound nucleus.

3. Modeling of spallation reactions

3.1. Characteristics of the two reaction stages

The collision-stage is very fast. The nucleon-nucleon collisions are estimated to occur in the order of 10 fm/c. After the primary collisions, the distorted nuclear system evolves towards the thermalisation of the nucleonic motion (≈ 100 fm/c). When the thermalisation is completed, the remnant nucleus can be considered to be a compound nucleus. The situation after the first-stage processes is fully described by the parameters of the compound nucleus. They define the starting point of the de-excitation process. The compound nucleus is characterized by composition in A and Z , thermal excitation energy, angular momentum, and linear momentum.

Once the thermalisation of the nucleonic motion is reached, the second stage starts, where the statistical de-excitation is treated. At first the system expands (≈ 100 fm/c). Depending on the temperature it can experience thermal instabilities and break-up into several pre-fragments or evolve as a single compound nucleus. Later on, the system starts its long (up to $\approx 10^7$ fm/c) sequential de-excitation process – consisting of small-nuclei, particle, and gamma emission – which eventually leads to the cold remnant fragment (experimentally observable). In case of heavy nuclei, in each de-excitation step fission is also a possible competitive decay channel.

3.2. Influence of the first stage on the final results

The de-excitation process wipes out most of the properties of the heated thermalised system. Most of the characteristics of the final residues are fingerprints of the de-excitation process. In *FIG 1*, it is shown the composition in A and Z of the compound nuclei as predicted by INCL4 and the experimentally observed final nuclei [8], presented on the chart of the nuclides, for the spallation of ^{238}U at 1 GeV. Nonetheless, the de-excitation process does not wash out all: The overall features of the final fragments are affected strongly by the output from the first-stage. Specifically: 1) The initial distribution of compound nuclei gives the starting point on the chart of the nuclides and it is reflected in the final production [9], 2) the thermal excitation energy influences the competition between the various decay channels, defines the volume of the system and its thermal instability (possibly leading to multifragmentation), 3) the acquired angular momentum has a strong influence on the fission process. On the contrary, linear momentum has no influence on the de-excitation process (yet it provides important signatures of the reaction mechanisms [10]). To clarify point 1), an example is presented in *FIG. 2-b*, where the experimental mass distribution of the residues produced in the reaction 1 A GeV ^{56}Fe on proton [10,11] is compared with two different calculations. The two calculations are based on two different distributions of remnants after the INC stage, coupled with ABLA07. The remnants distributions are presented in *FIG. 2-a*:

The solid curve gives the prediction of INCL4, the dashed curve is an artificially modified distribution; to both distributions – solid and dashed – correspond the same excitation-energy and angular-momentum distributions (cf. FIG. 3). Fig.2-b indicates clearly that the initial distribution of compound nuclei is reflected in the final production. To a further discussion on point 2), please cf. section 2.3 of ref. [12], where it is shown that extending the range of remnants excitation energy to higher values will result in a longer chain of spallation residues. To exemplify point 3), in FIG 2-c, the experimental Z distribution of the products of 1 A GeV²⁰⁸Pb on protons [13] is compared with two results of INCL4+ABLA07. The solid curve represents the unbiased calculation, while the dashed one was obtained by artificially doubling the angular momentum of the remnants after the INC.

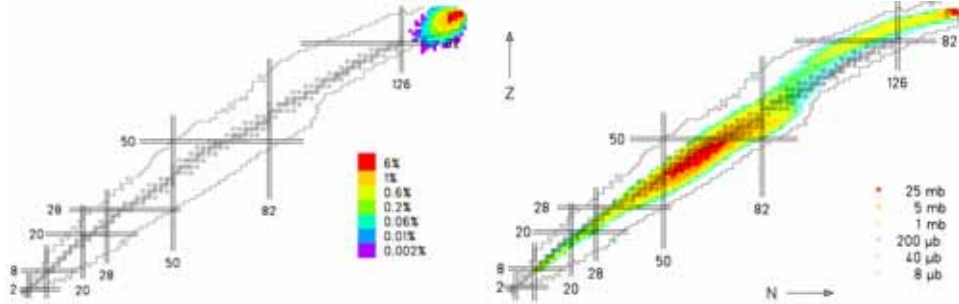


FIG. 1. Left: Population of compound nuclei formed after the first-stage of the reaction $1\text{ GeV } p + {}^{238}\text{U}$ predicted by INCL4. Right: Final nuclei produced in the same reaction, measured at GSI [8].

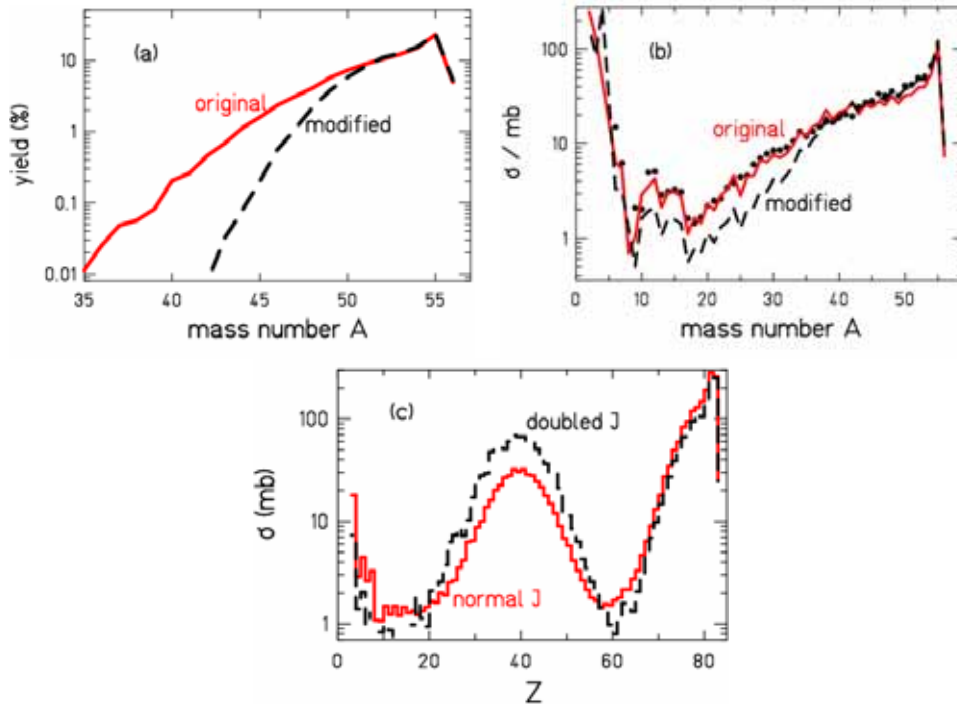


FIG. 2. (a) Remnants after the INC stage for the reaction $1\text{ GeV } p + {}^{56}\text{Fe}$, as predicted by INCL4 (solid curve). The dashed curve is an artificially modified distribution.

(b) Corresponding final mass distributions after the de-excitation stage, calculated with ABLA07. The dots are the experimental data, taken at GSI [10,11].

(c) Simulations of the reaction $1\text{ GeV } p + {}^{208}\text{Pb}$ with INCL4+ABLA07 (solid curve). The dashed curve is obtained by artificially doubling the angular momentum J of the remnants after the INC stage.

4. Results

In this section, we discuss the results of INCL4+ABLA07, ISABEL+ABLA07, and ABRABLA07. We analyze the spallation of three systems at 1 GeV: 1) ^{56}Fe – a key case to study the evaporation process –, 2) ^{208}Pb – a key case to study the competition between fission and evaporation –, and 3) ^{238}U – a key case to study the fission process.

4.1. Reaction 1 GeV $p + ^{56}\text{Fe}$

In FIG 3, the main characteristics of the remnants after the collision stage are shown. The results from the three reaction models are presented. In the left upper panel, the production of remnants is presented, normalised to 100. All models overlap in the region $50 \leq A \leq 55$, where most of the production is predicted. INCL4 and BURST coincides for masses larger than $A=47$, which make up 98.9% of the total production. The predictions of the mean Z of the isobaric distributions (right upper panel) coincide for the three models. The average excitation energy per nucleon (left lower panel) predicted by BURST has a slightly different tendency than INCL4 and ISABEL ones. Concerning the average angular momentum (right lower panel), INCL4 predicts higher values with respect to BURST and ISABEL, however the statistical fluctuations are rather high. In FIG 4, we show the results after coupling the three models with ABLA07. The yields of the final products are presented as a function of their atomic number Z (right upper panel) and mass number A (left upper panel) and compared with the experimental data taken at GSI, Darmstadt [10,11]. The results of INCL4-ABLA07 and ABRABLA07 practically coincide; they are overall very good. ISABEL-ABLA07 predicts too few deep-spallation products, probably reflecting the remnant yield distribution and too few intermediate-mass fragments IMF (approx. $A < 25$) probably due to low number of remnant with high excitation energy. In the lower panels, the ratios of the experimental cross-sections to the model-predicted ones are presented on the chart of the nuclides.

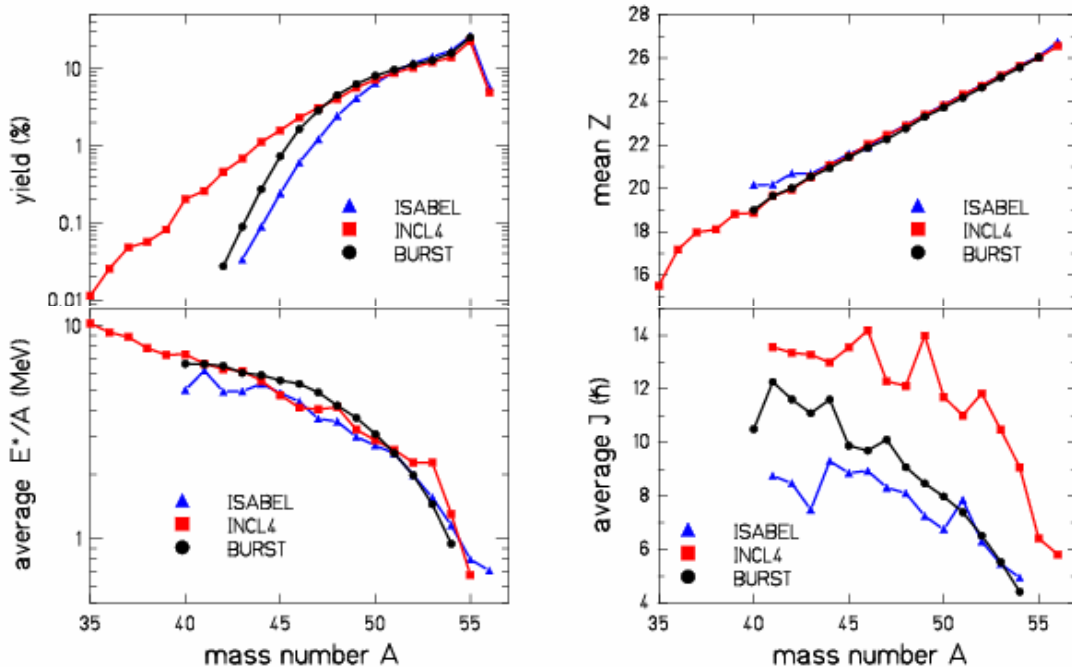


FIG. 3. Simulations of the collision stage for the reaction $1\text{ GeV } p + ^{56}\text{Fe}$ performed with ISABEL, INCL4, and BURST. The four panels present the main characteristics of the remnants after the collision stage as a function of the remnant mass A . See text for details.

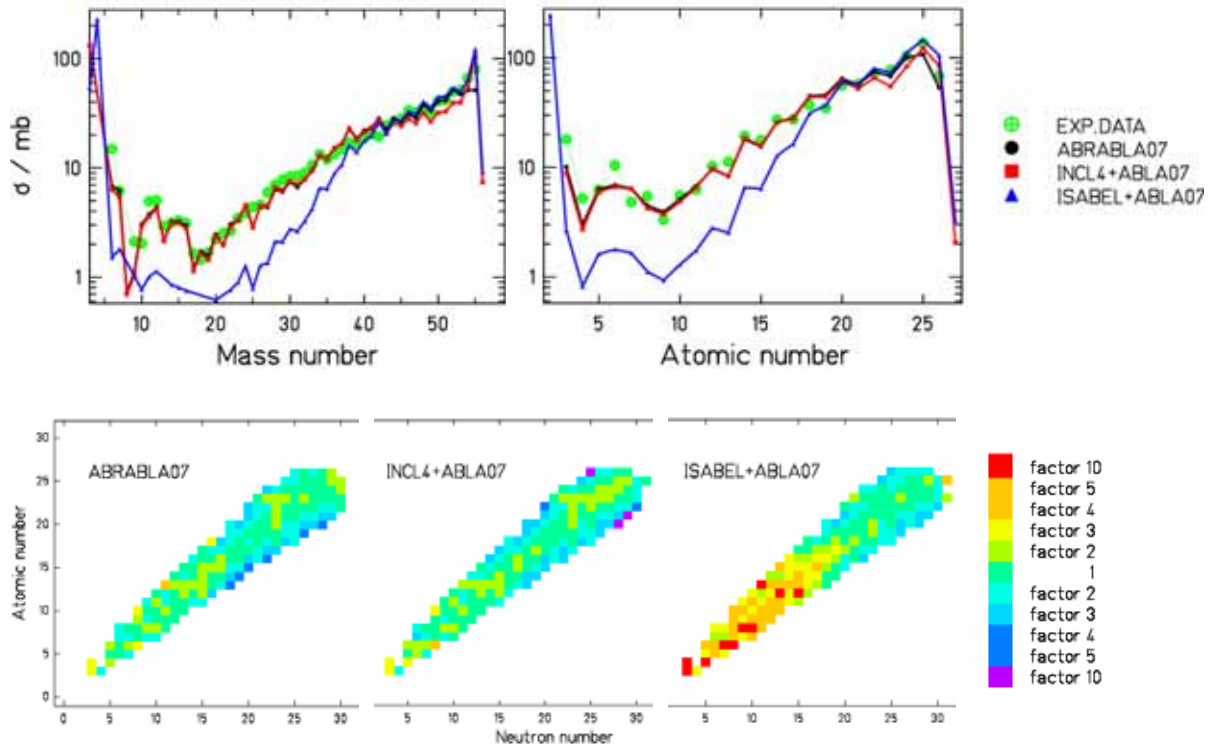


FIG. 4. Up: Production cross-sections for the reaction $1\text{ GeV } p + {}^{56}\text{Fe}$ as predicted by ISABEL-ABLA07, INCL4-ABLA07, and ABRABLA07. The experimental data are from [10,11]. Down: ratio of the experimental cross-sections to the model-predicted ones, presented on the chart of the nuclides.

4.2. Reaction $1\text{ GeV } p + {}^{208}\text{Pb}$

In a similar way as in section 4.1, we present here the results for the reaction $1\text{ GeV } p + {}^{208}\text{Pb}$. In FIG. 5 the results after the collision stage are presented as a function of the remnant mass.

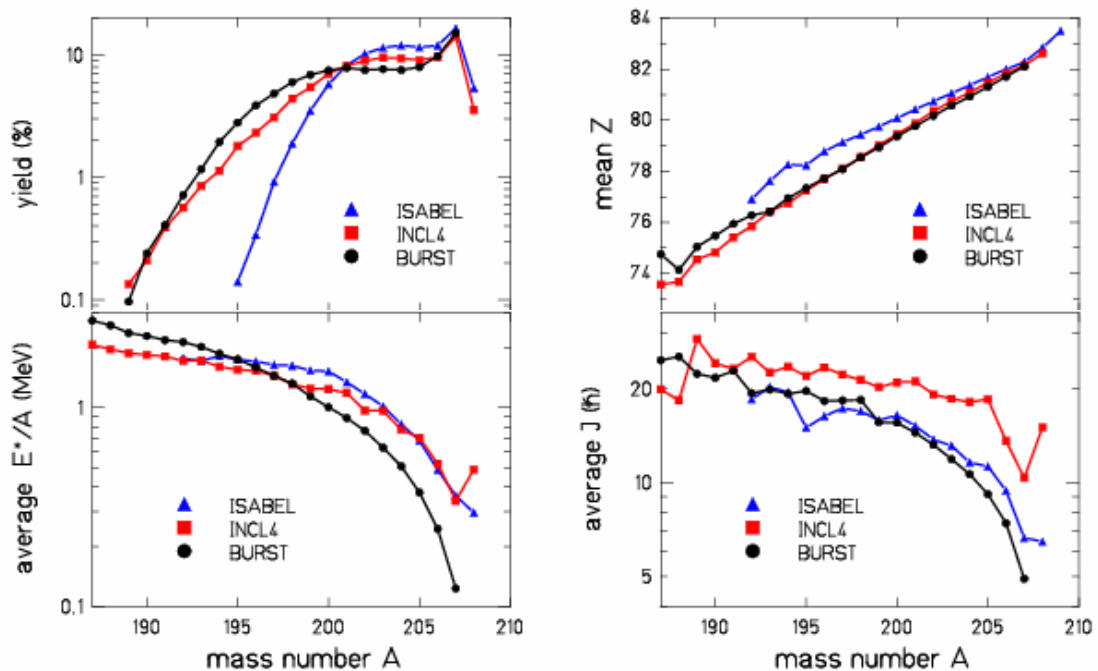


FIG. 5. Simulations of the collision stage for the reaction $1\text{ GeV } p + {}^{208}\text{Pb}$ performed with ISABEL, INCL4, and BURST. The four panels present the main characteristics of the remnants after the collision stage as a function of the remnant mass A . See text for details.

One can notice appreciable differences in the remnant yields among the three codes: the production of remnants with $A \geq 201$ amounts to 63%, 72%, and 87% as predicted by BURST, INCL4 and ISABEL, respectively. Differences are also visible in the mean Z , average excitation energy E^* and average angular momentum J of the remnants. As in the previous case, the E^* predicted by ABRA has a different tendency than the others. Again, INCL4 predicts the highest J . In FIG. 6, the results for the final products, after the de-excitation with ABLA07, are presented. ABRABLA07 reproduces at the best the experimental data, taken at GSI, Darmstadt [13]. INCL4-ABLA07 results are also good, although fission products are overestimated by about a factor 2. This discrepancy could be connected to higher J and higher E^* of the remnants predicted by INCL4. Similar consideration could be driven for ISABEL-ABLA07 fission products. As in the previous case, ISABEL-ABLA07 shows the highest discrepancies for deep-spallation products.

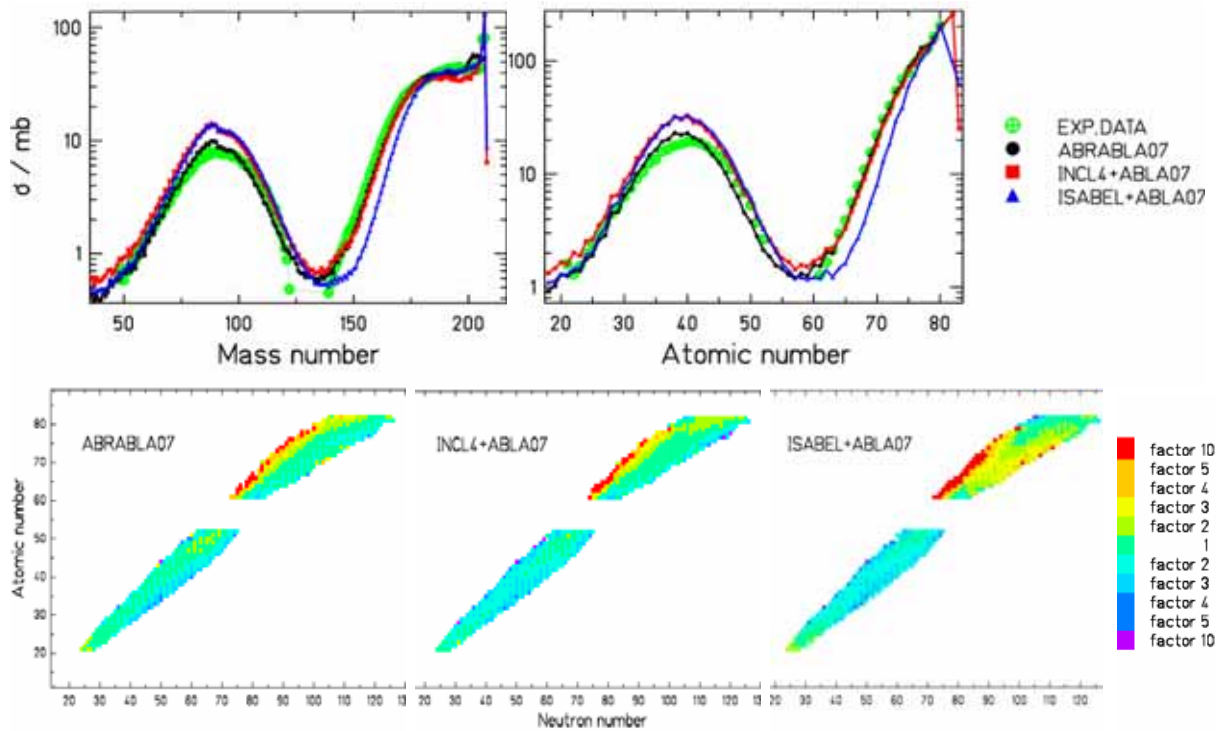


FIG.6. Up: Production cross-sections for the reaction $1\text{ GeV } p + {}^{208}\text{Pb}$ as predicted by ISABEL-ABLA07, INCL4-ABLA07, and ABRABLA07. The experimental data (dots) are from [13]. Down: ratio of the experimental cross-sections to the model-predicted ones, presented on the chart of the nuclides.

4.3. Reaction $1\text{ GeV } p + {}^{238}\text{U}$

Very similar considerations as for the previous case can be driven for the remnants of the reaction $1\text{ GeV } p + {}^{238}\text{U}$, presented in FIG. 7. The final residues are presented in FIG. 8, compared to the experimental data taken at GSI, Darmstadt [8]. Contrary to the ${}^{208}\text{Pb}$ case, where fission occurs only at higher E^* , here fission is dominant at almost all energies. The fission products are very well reproduced in all three cases, demonstrating the validity of the fission model in ABLA07. Please note that also the IMF production is very well reproduced, indicating a harmonic description of fission and evaporation processes [5]. Larger discrepancies are found in the spallation residues, especially in the case of deep-spallation products predicted by ISABEL-ABLA07.

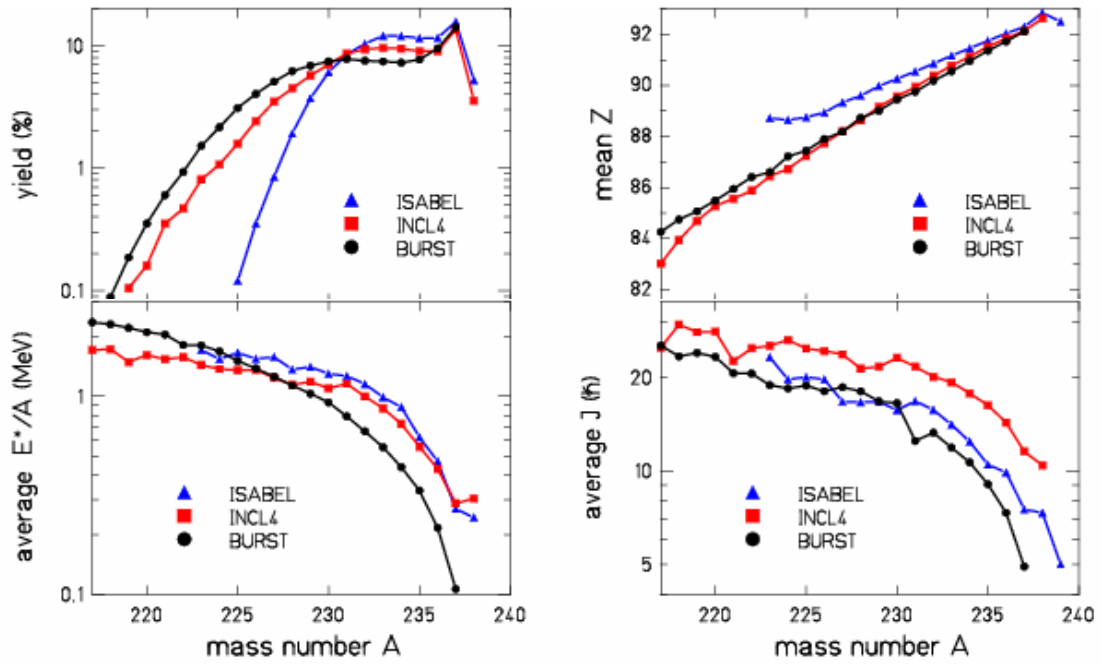


FIG. 7. Simulations of the collision stage for the reaction $1\text{ GeV } p + {}^{238}\text{U}$ performed with ISABEL, INCL4, and BURST. The four panels present the main characteristics of the remnants after the collision stage as a function of the remnant mass A . See text for details.

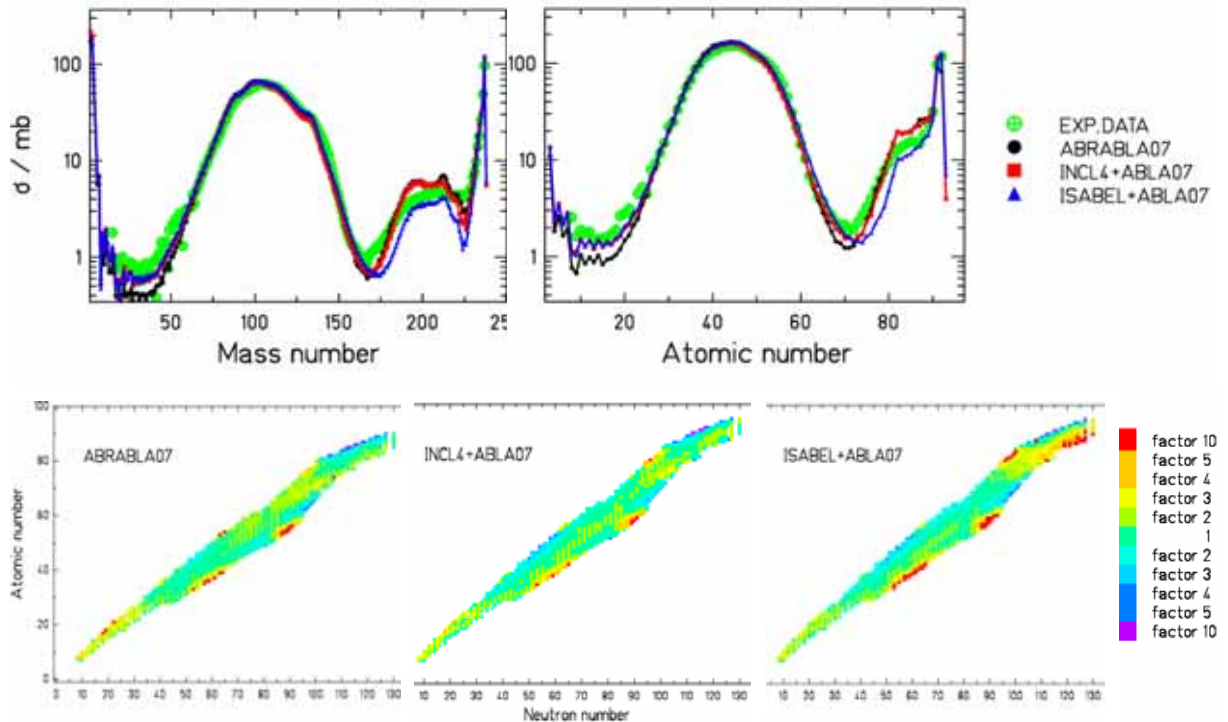


FIG. 8. Up: Production cross-sections for the reaction $1\text{ GeV } p + {}^{238}\text{U}$ as predicted by ISABEL-ABLA07, INCL4-ABLA07, and ABRABLA07. The experimental data are from [8]. Down: ratio of the experimental cross-sections to the model-predicted ones, presented on the chart of the nuclides.

6. Conclusions

In this work, we coupled the de-excitation code ABLA07 [2] to three different models of the collision stage: INCL4 [3], ISABEL [4], and BURST [5,6]. We analyzed the spallation at 1

GeV of three systems: ^{56}Fe , ^{208}Pb , and ^{238}U . The experiments were performed at GSI, Darmstadt [8,10,11,13].

The discrepancies among the different variables (yield, average atomic number, excitation energy, and angular momentum), which characterize the remnants predicted by the three models, amount in most cases to about a factor 2. The following de-excitation process does not wash out these differences. This indicates that adapting a de-excitation model to a given INC model, such to provide the best final results when combined together, does not automatically assure high predictive power in regions not tested before. Larger cross checks and benchmark with many experimental data are therefore needed to fix the various models.

ACKNOWLEDGMENTS

We wish to thank Davide Mancusi for calculating the distributions of remnants predicted by INCL4 and ISABEL. We acknowledge the financial support of the European Community under the FP6 Integrated Project EUROTRANS Contract no. FI6W-CT-2004-516520 and “Research Infrastructure Action – Structuring the European Research Area” EURISOL DS Project Contract no. 515768 RIDS. The EC is not liable for any use that may be made of the information contained herein.

REFERENCES

- [1] Proceedings of the Advanced Workshop on Model Codes for Spallation Reactions, ICTP Trieste, Italy, 4-8 February 2008. D. Filges, S. Leray, Y. Yariv, A. Mengoni, A. Stanculescu, and G. Mank Eds., IAEA INDC(NDS)-530, Vienna, August 2008. <http://www-nds.iaea.org/reports-new/indc-reports/indc-nds/indc-nds-0530.pdf>
- [2] A. Kelić, M.V. Ricciardi, K.-H. Schmidt, “ABLA07 - Towards a complete description of the decay channels of a nuclear system from spontaneous fission to multi-fragmentation”, pg. 181-221 of ref. [1].
- [3] A. Boudard, J Cugnon, “INCL4–The Liege INC model for high-energy hadron-nucleus reactions”, pg. 29-50 of ref. [1].
- [4] Y. Yariv, “ISABEL–INC model for high-energy hadron-nucleus reactions”, pg. 15-28 of ref. [1].
- [5] M.V. Ricciardi et al., Phys. Rev, C 73 (2006) 014607.
- [6] S. Lukić, K.-H. Schmidt, F. Vives, to be published.
- [7] J.-J. Gaimard, K.-H. Schmidt, Nucl. Phys. A 531 (1991) 709-745
- [8] P. Armbruster et al., Phys. Rev. Lett. 93 (2004) 212701 and therein references.
- [9] X. Campi and J. Hüfner, Phys. Rev. C 24 (1981) 2199-2209.
- [10] P. Napolitani et al., Phys. Rev. C 70 (2004) 054607
- [11] C. Villagrasa-Canton et al., Phys. Rev. C 75 (2007) 044603
- [12] M. V. Ricciardi et al., Europ. Phys. Jour. A 150 (2007) 321-324.
- [13] T. Enqvist et al., Nucl. Phys. A 686 (2001) 481-524.